Application of steered molecular dynamics (SMD) to study DNA–drug complexes and probing helical propensity of amino acids

2005 J. Phys.: Condens. Matter 17 S1627

(http://iopscience.iop.org/0953-8984/17/18/018)

INSTITUTE OF PHYSICS PUBLISHING JOURNAL OF PHYSICS: CONDENSED MATTER

J. Phys.: Condens. Matter **17** (2005) S1627–S1640 doi:10.1088/0953-8984/17/18/018

Application of steered molecular dynamics (SMD) to study DNA–drug complexes and probing helical propensity of amino acids

Marek Orzechowski[1] **and Piotr Cieplak**[2]

[1] Faculty of Chemistry, Warsaw University, 1 Pasteura Street, Warsaw, 02-093, Poland
[2] Accelrys Incorporated, 9685 Scranton Road, San Diego, CA 92121, USA

E-mail: morzech@tiger.chem.uw.edu.pl and pcieplak@accelrys.com

Received 26 October 2004, in final form 26 October 2004
Published 22 April 2005
Online at stacks.iop.org/JPhysCM/17/S1627

Abstract

We present the preliminary results of two computer experiments involving the application of an external force to molecular systems. In the first experiment we simulated the process of pulling out a simple intercalator, the 9-aminoacridine molecule, from its complex with a short DNA oligonucleotide in aqueous solution. Removing a drug from the DNA is assumed to be an opposite process to the complex formation. The force and energy profiles suggest that formation of the DNA–9-aminoacridine complex is preferred when the acridine approaches the DNA from the minor groove rather than the major groove side. For a given mode of pulling the intercalation process is also shown to be nucleotide sequence dependent.

In another computer experiment we performed a series of molecular dynamics simulations for stretching short, containing 15 amino acids, helical polypeptides in aqueous solution using an external force. The purpose of these simulations is to check whether this type of approach is sensitive enough to probe the sequence dependent helical propensity of short polypeptides.

1. Introduction

Recently, the rapid development of modern experimental techniques such as the AFM (atomic force microscope) or so-called optical tweezers has enabled the direct manipulation of a single molecule on the atomic level. Such techniques are mainly applied to biologically important molecules of living organisms. The ability to manipulate large molecules on an atomic scale has encouraged experimentalists to reproduce biological phenomena such as strand separation in double stranded DNA [1, 2], stretching DNAs and RNAs [3–5], complex formation between various proteins and ligands [6–8], as well as stretching elastic proteins such as titin [9, 10]. Examples of review papers covering both experimental and theoretical aspects of studies

involving force induced manipulation of molecules are those by Strick *et al* [11], Leckband [12] and Bustamante *et al* [13].

Many experimentally studied systems have also been investigated using theoretical methods such as molecular mechanics (MM) and molecular dynamics (MD). Those methods can be used to simulate systems with full atomic representation and are able to provide additional information that is not easily available from experimental methods. Classical molecular dynamics methods can only be used to simulate systems under equilibrium conditions. To be able to simulate molecules under non-equilibrium conditions, caused for example by tensile forces, the classical methods required the implementation of new algorithms. An example of such implementations has been described by Izrailev *et al* in 1998 [14].

The main computational technique used to study molecules under a tensile force is a recently developed method called steered molecular dynamics (SMD). It is suitable for simulating non-equilibrium processes or processes that have a long time of duration; for example, it could be used for modelling helix to coil transitions, mechanics of proteins in muscles, folding–unfolding nucleic acid strands, disrupting protein–ligand complexes and many other processes. The introduction of the SMD method has allowed the simulation of dynamic processes such as the dissociation of biotin from avidin and streptavidin [15, 16], unbinding of retinal from bacteriorhodopsin [17], and the extraction of lipids from membranes [18]. In the SMD technique the substantial conformational or configurational changes in the desired direction are induced by applying an external force. Without such an external force the classical molecular dynamics simulations would need enormously long computational time to achieve the same effect or the effect would not be observed at all. Thus, the SMD technique allows the simulation of various phenomena in a reasonably short time. Also, the SMD technique provides full atomistic details of the simulated process, e.g. solvent rearrangement in explicit solvent calculations, and details of geometry changes, which are not usually available from experimental techniques. The computer experiments of Isralewitz *et al* [17] and Stepaniants *et al* [18] have been conducted in a way similar to the experimental conditions, which made direct comparison of the results between those two approaches possible. In many cases the agreement between experiment and simulations was remarkably good; for example in the work of Grubmüller *et al* [16] on biotin–streptavidin complexes.

Recent development of theories, such as the introduction of Jarzynski's equality [19, 20] and further advancement in modern experimental techniques has resulted in accurate and flexible tools for better interpretation of both experimental and theoretical results. They were successfully applied to interpret the unfolding of the titin Ig domain [21], mechanical stretching of RNA [22] and for calculating the potentials of the mean force from steered molecular dynamics simulation [23].

In the first part of the paper we present the results of our calculations for the DNA and 9-aminoacridine (9-AA) complex, in which ligand intercalating between nucleic acid base pairs has been pulled out of the complex. All simulations have been performed in aqueous solution. To our knowledge no one has tried to apply the SMD technique to study nucleic acid–drug complexes in explicit or implicit solvent models. This type of computer simulation provides detailed information about the energetics and forces acting on the microscopic level that govern the process of specific DNA–drug complex formation. Additionally, we gain information about the role that water molecules play in the intercalation process.

In the second part of the paper we describe our attempt to study the sequence dependent α-helix to coil transition in short polypeptides caused by an external force. The α-helices are important components of protein structures. Due to their importance in protein folding

studies, α-helices became interesting systems for experimental manipulations. For example, Lantz *et al* [24] managed to evaluate the stiffness of spring-like helices and determined the energy of hydrogen bonds in the backbone of the helix by employing the tip of an AFM. In our simulations we tried to evaluate the relative helical propensities of different amino acids in a way similar to the Lantz *et al* experiments on α-helices performed using the AFM technique.

2. Intercalation

2.1. Introduction

The small molecules that are groove binders or intercalate into the DNA become a vivid subject of many studies because of their importance in anti-tumour [25] and, recently, in anti-malarial treatment [26]. Intercalating ligands usually exhibit strong preference to bind to a specific nucleotide sequence. The main goal of studies on intercalation phenomena is predicting the stability of the complexes and selectivity of intercalators with respect to the nucleotide sequence. Most of those experiments focused on solving structures of the complexes and determining appropriate binding constants. On the other hand no detailed information exists on thermodynamic and kinetic descriptions of the processes leading to the formation of such complexes. The intercalation process is not very well understood and is not yet described on the atomic level.

One of the smallest intercalators is the acridine molecule. In 1961 Lerman proposed a model of acridine intercalation into DNA [27]. Since then, for more than 40 years, acridine and its derivatives have been the subject of many other studies.

Along with experiments, theoretical studies have also been conducted for various intercalators. For example, in 1979 Nuss *et al* [28] applied an empirical potential energy function to examine the interaction of intercalating ligands with small nucleic acid components in order to determine the origin, nature and magnitude of the forces that govern the stability of such complexes. There were also other attempts to calculate binding free energies using the free energy perturbation method. It was applied to study the sequence dependent stability of daunomycin and 9-aminoacridine complexes with hexamer d(CpGpTpApCpG) [29]. Although calculations at that time were done without explicit solvent the results revealed quite good agreement with experimental results, that were also proved by later investigations; we will mention this later. The main conclusion of the computer simulations was that acridine prefers GC-rich regions over AT sequences of DNA.

In 1995 Crenshaw *et al* [30] studied the binding free energies of small intercalators in complexes with DNA. They estimated that the binding ΔG of 9-aminoacridine to calf thymus DNA is equal to -7.7 ± 0.2 kcal mol^{-1}. Other intercalators exhibit binding ΔG that ranges from -6.7 kcal mol^{-1} for simple intercalators such as ethidium in complex with calf thymus DNA, up to -15.3 kcal mol^{-1} for larger molecules, such as WP631 interacting with herring sperm DNA. The value of binding ΔG for a given intercalator depends on the salt concentration, DNA sequence and other conditions specific to the given experiments.

In this study we would like to describe the results of application of the SMD method to 9-aminoacridine–DNA complexes, where the external force is applied to the ligand molecule in order to pull it out from the intercalation site. The 9-AA is an aromatic ligand (see figure 1), which due to its planarity may intercalate between nucleic acid base pairs of DNAs and RNAs.

In the nucleic acid database [31] and protein data bank [32] there are only a few structures of nucleic acid with acridine derivatives. One of them is a complex of 9-AA with RNA and the others are complexes of DNA with various derivatives of acridine, for example 9-amino-[N-(2-dimethyloamino)-ethyl]acridine-4-carboxamide (9-amino-DACA). The examination of

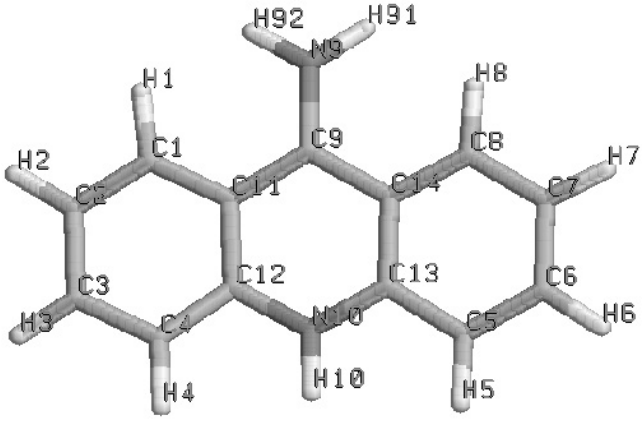

Figure 1. The structure of 9-aminoacridine (9-AA).

various crystal structures of 9-AA derivatives suggests that 9-aminoacridine most probably intercalates from the minor groove of the DNA. In most cases of the known structures, acridine is located between the terminal base pairs of nucleic acid at the end of DNA. In one case, a complex 1G3X [33], the acridine derivative intercalates between the middle base pairs of the DNA dodecamer. The structural parameters for this complex, especially the size of the intercalation cavity, are very similar to those observed in our structure that have been used for calculations.

The stability of these complexes is usually attributed to the π interactions between aromatic rings of the nucleic bases and acridine molecule. In the case of acridine derivatives, additional stabilization can result from interaction of the acridine side chain with DNA. In most cases it is located in the major groove and favourably interacts electrostatically with neighbouring nucleic bases. The absorbance spectroscopy studies of Crenshaw *et al* [30] have shown that intercalators prefer CG rich sequences and enter the binding site through the minor groove. However, Adams *et al* [34] demonstrated that in the crystallographically determined structures the side chain of the 9-amino-DACA molecule can also be located in the major groove. This suggests that the ligand can enter the intercalation site through the major groove as well. Those two experimental findings show that the nature of intercalation is still not very well understood. To make the situation even more complicated, it is still not quite clear whether 9-AA is a pure intercalator or groove binder as well [35]. The above issues, including the role of solvation during the intercalation process, can be studied by the SMD simulation method, and some of them will be addressed below.

2.2. Results of the SMD simulations of the intercalation process

We performed molecular dynamics simulations for the DNA–9-AA intercalation complex in aqueous solution during which the 9-aminoacridine molecule has been pulled out of the DNA with a constant speed. We applied the techniques similar to the steered molecular dynamics (SMD) method described by Lu and Schulten [36] using the AMBER 6 package [37]. We applied this approach to a model system consisting of DNA d(GAA**XY**TTC), where **XY** is **AT** or **CG**, and the 9-aminoacridine molecule, which intercalates between the **XY** nucleotides. An example of one of such structure is shown in figure 2.

In order to perform the pulling experiment an artificial atom BA has been attached to the H10 or N9 atom of the 9-AA molecule depending on the pulling direction (see figure 1).

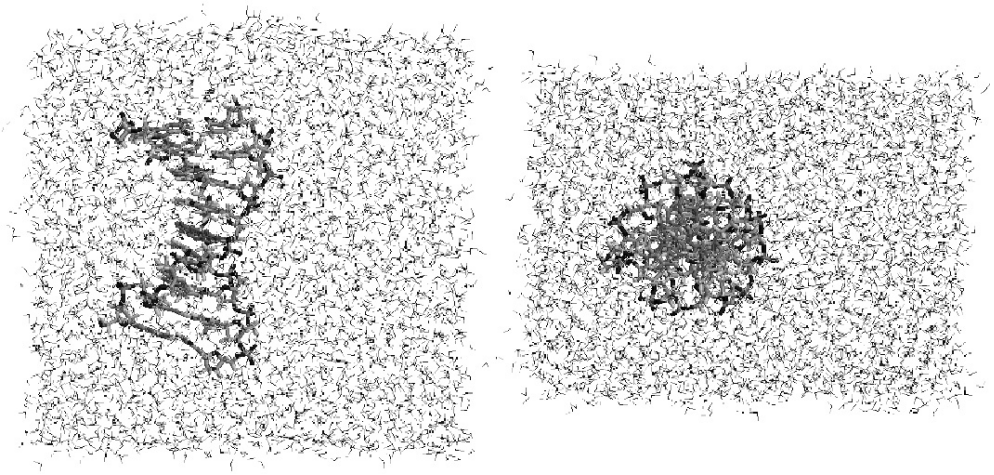

Figure 2. Complex of d(GAACGTTC) with 9-aminoacridine, solvated asymmetrically in a box of water molecules, after minimization and 190 ps of equilibration. The system is prepared for pulling 9-AA through the minor groove. The side and the top view of the complex are on the left- and right-hand side of the figure, respectively.

If pulling proceeded through the minor groove the BA atom was attached to the H10 atom, whereas it was attached to the N9 atom for pulling out on the major groove side. The bond between BA and a real atom has an equilibrium length of 2 Å and is described by a harmonic term with the force constant equal to 6 kcal mol^{-1} $Å^{-2}$ (417.1 pN $Å^{-1}$). The actual pulling experiment was performed in such a way that atom BA was moved from one position into another by 0.05 Å along the line perpendicular to the main axis of the DNA. At each new position the atom BA was positionally constrained and 100 fs of molecular dynamics was performed allowing the elongated probing bond to relax. The fluctuation of the bond length between BA and the real atom was measured in order to determine the forces needed to pull 9-aminoacridine out of the intercalation site. The whole process was finished when the drug was totally removed from the intercalation site and BA was displaced from the initial position by 50 Å. However, the displacement of the BA atom by 25 Å seemed to be sufficient for the purpose of analysis. The step by step repositioning of the BA atom is equivalent to a constant velocity movement with speed equal to 50 m s^{-1} (or equivalently 0.5 Å ps^{-1}), which is a few orders of magnitude larger than the velocities applied in a real experiment. Changing the position of the artificial BA atom used in the pulling experiment was done by an additional script outside the molecular dynamics program.

By measuring the relative changes in the length of the probing bond between BA and H10 or N9, and by performing some additional energetic analysis, we were able to determine the appropriate force, energy and free energy profiles for the process of removing the 9-aminoacridine molecule from the DNA through the major (pulling by the N9 atom) and minor (pulling by the H10 atom) groove. Removing the drug from the DNA is assumed to be an opposite process to the complex formation.

The initial geometries for the molecular dynamics simulations were built based on available information for acridine derivatives and DNA complexes, as well as using crystallographically determined structure of short DNA sequences in complex with the chromophore part of the actinomycin molecule as a template [38]. In our computational experiments we applied standard parm99.dat force field parameters [39]. The atomic charges for the 9-aminoacridine

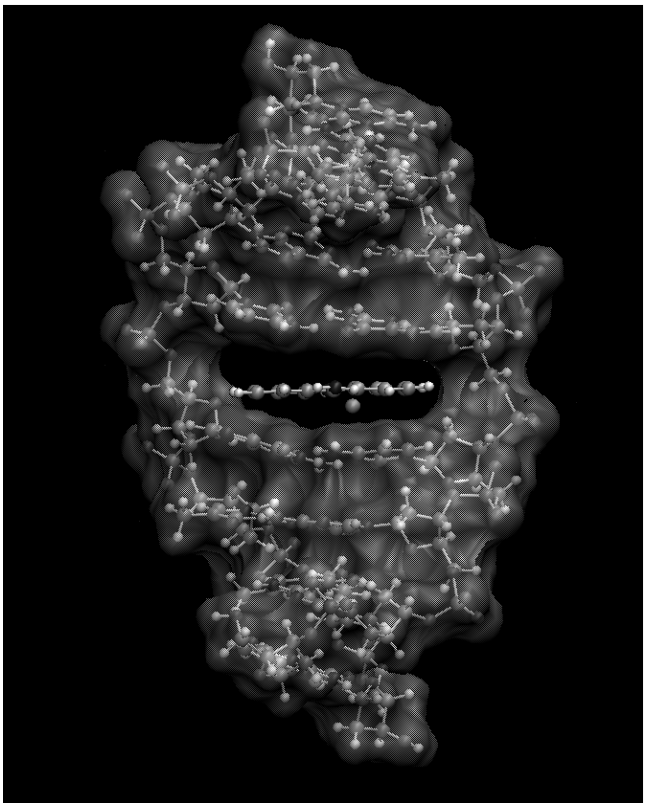

Figure 3. Image showing the intercalation cavity for the B-DNA and 9-AA complex. The semi-transparent region represents the solvent accessible surface area of B-DNA. The lone sphere located close to 9-AA represents the BA atom. The bond between BA and an atom in 9-AA is not shown.

molecule were calculated using the standard RESP procedure [40]; the other force field parameters were determined using optimized geometries from *ab initio* HF/6-31g* geometry optimization by the Gaussian98 program [41].

All simulations were performed in a periodic box of TIP3P [42] water molecules. The DNA–9-AA complex was initially situated close to one side of the box and the box size was chosen so as to accommodate the fully solvated DNA and 9-aminoacridine molecule separated by a distance of 50 Å at the end of pulling experiment. The number of water molecules ranged from 4324 to 4436 and the size of the water box was $72 \times 56 \times 42$ Å^3. An example of one such initial structure without the solvent is shown in figure 3. We performed NpT molecular dynamics simulations, at $p = 1$ atm and $T = 300$ K, using 9.0 Å cutoff for non-bonded interaction and the PME method for the electrostatic energy calculation.

The plots in figure 4 display the force profiles obtained from direct evaluation of Hooke's law for a harmonic spring, $F = -k(l - l_0)$, where F is a force, k is a force constant and l, l_0 are the current length and equilibrium length of a spring. In our case l_0 was set to be 2.0 Å and k is equal to 6 kcal mol^{-1} Å^{-2}. We have chosen such a value based on the computational experiments of Lu *et al* [36] to maintain the stiff spring regime in our calculations. Simulations have been performed for four different cases, in which acridine was initially located between AT or CG base pairs and the pulling was performed through the minor or the major groove. For each case we performed 10 simulations that differed by the initial atomic velocities distribution.

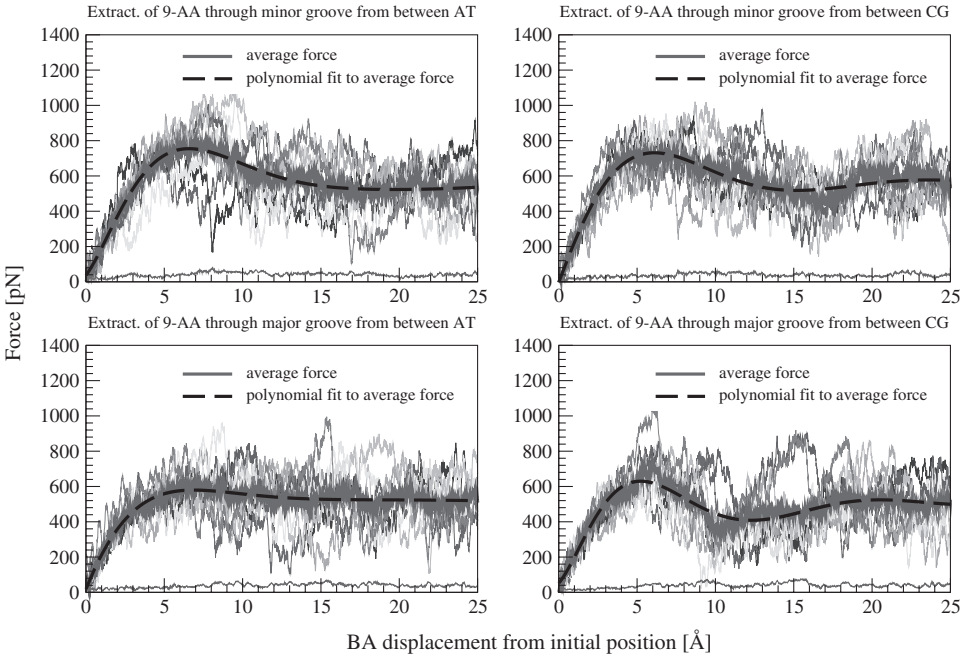

Figure 4. Force profiles obtained from all pulling experiments for the B-DNA and 9-AA complex. The thin line at the bottom of each plot represents the standard deviation of average force.

The results have been averaged out and are presented in figure 4. All plots in figure 4 exhibit a similar tendency. At the initial stage of pulling the force substantially increases to achieve the maximum value and after that decreases, slowly stabilizing and then remaining at an almost constant level during the rest of the pulling experiment. Such a behaviour suggests that it is possible to determine the point at which the DNA–9-AA complex is disrupted and the 9-AA becomes totally solvated. The maximum value of the force in each case is found to be at the location of BA that is around 5–6 Å away from its initial position. The largest force is needed for pulling 9-AA through the minor groove from the AT intercalation site. Less force, compared to the AT-minor groove pulling, is required for pulling 9-AA from the CG site through the minor groove and then even less for pulling from the CG site through the major groove. Finally, the least force is required for pulling the 9-AA from the AT site through the major groove. When 9-aminoacridine is pulled beyond 10 Å the force profiles do not change substantially, and can be ascribed to the situation in which 9-AA is pulled with its own hydration shell through the bulk water with a constant velocity. In this case the only factor causing the force to have a non-zero value is the viscosity of the solvent.

Table 1 summarizes all the numerical results derived from the force profiles averaged over ten simulations for each case. The first two columns of this table present the maximum force (in pN) calculated directly from bond elongation and the maximum force obtained from the polynomial fit of tenth order to the directly calculated forces. The third column contains the results of work (in kcal mol^{-1}) performed for displacing BA up to 10 Å from its initial position, which is calculated as an integral over the average force. The fourth column is the work determined as an integral over the fit to directly calculated forces. The last column contains ΔG obtained from the Jarzynski formula, as described below. The work in table 1, except the information about the binding free energy, also carries information about irreversible work. In order to be able to compare the relative stabilities of different complexes we need to

Table 1. Table showing maximum values of force and work as an integral of force over BA displacement. The force was calculated directly from the elongation of the bond between BA and N9 (or H10) atoms in acridine. In parentheses the BA displacement from the centre of the intercalation site is reported where the maximum value of the force occurs. For each set of data a polynomial curve was fitted. The details of the fitted curves are also presented. Work marked with § is calculated as an integral over the average force, and that marked with ♯ is an integral of the fit over the BA displacement. ΔG is a free enthalpy calculated from Jarzynski's equality.

	Max average force (pN)	Max fit (pN)	Work § (kcal mol^{-1})	Work ♯ (kcal mol^{-1})	ΔG (kcal mol^{-1})
AT minor groove	799.63 ± 50.89 (7.07 Å)	754.60 (6.57 Å)	83.37 ± 5.61	82.87	71.79
AT major groove	625.26 ± 44.28 (8.77 Å)	579.71 (6.87 Å)	67.80 ± 4.52	67.78	60.69
CG minor groove	748.59 ± 32.51 (5.50 Å)	731.36 (6.09 Å)	81.81 ± 4.78	82.22	72.35
CG major groove	724.30 ± 48.38 (6.07 Å)	629.98 (5.22 Å)	69.18 ± 4.84	68.91	59.79

assume that the irreversible contribution is very similar in all cases. If we assume that more work is required to disrupt a more stable complex, then the largest work is done for extracting 9-AA through the minor groove from the site between AT, which seems to be the most stable complex. However, close to that is the case in which 9-AA is pulled from the CG site through the minor groove. Significantly less work is required to extract 9-AA from between CG and then AT, both through the major groove. If we assume that irreversible work is done to the same amount for all cases, and that the hysteresis for all systems is the same, we can conclude that complexes of 9-AA are created through the minor groove. On the other hand, the sequence dependency, i.e. the preference of the 9-AA to intercalate preferably between CG over the AT sequences, is not well reproduced. However, comparison of the fourth or fifth column in table 1 shows that the differences in the values of work between AT and CG through the minor groove and between AT and CG through the major groove are very small. Further analysis is required to explain this effect, which is possibly kinetic in origin.

The last column of table 1 shows the results for calculated binding free energies, ΔG (in kcal mol^{-1}), using Jarzynski's formula: $\exp[-\beta \Delta G(z)] = \lim_{N\to\infty} \langle \exp[-\beta w_i(z, r)] \rangle_N$. In our case the value of N, which is the number of simulations, is equal to 10. As we can see in table 1 Jarzynski's equation gives values of ΔG suggesting that the complex of 9-AA intercalating between CG is slightly more difficult to disrupt through the minor groove than the complex with 9-AA between AT in the same direction. These results shows better agreement with experimental findings. We expect that larger N and initiating simulations from different starting orientations of the intercalator in the binding site would yield more reliable results.

Additionally, we performed a hydration coordination analysis of the trajectories generated in the pulling experiment. In figures 5 and 6 we present the hydration coordination numbers for N9 and N10 (to which H10 is connected) atoms of 9-aminoacridine molecule as a function of pulling distance. The average coordination number is marked with a thick black line in each case. The solvation pattern clearly shows how the two atoms, N9 and N10, located on the opposite side of the 9-aminoacridine molecule become hydrated during the pulling experiment. When pulling is performed through the minor groove the N10 atom is immediately solvated but the N9 atom, located on the major groove site, has to be desolvated first in order to be pulled through the interior of the intercalation cavity. This desolvation effect occurs in the range between 5 and 8 Å of the pulling coordinate. When the N9 atom is in the middle of the cavity its hydration coordination number decreases approximately to 1, which means that only one water molecule attached to the 9-aminoacridine N9 atom has been pulled together through the intercalation site. A similar situation occurs when the pulling experiment is performed through the major groove, but the roles of N10 and N9 are reversed.

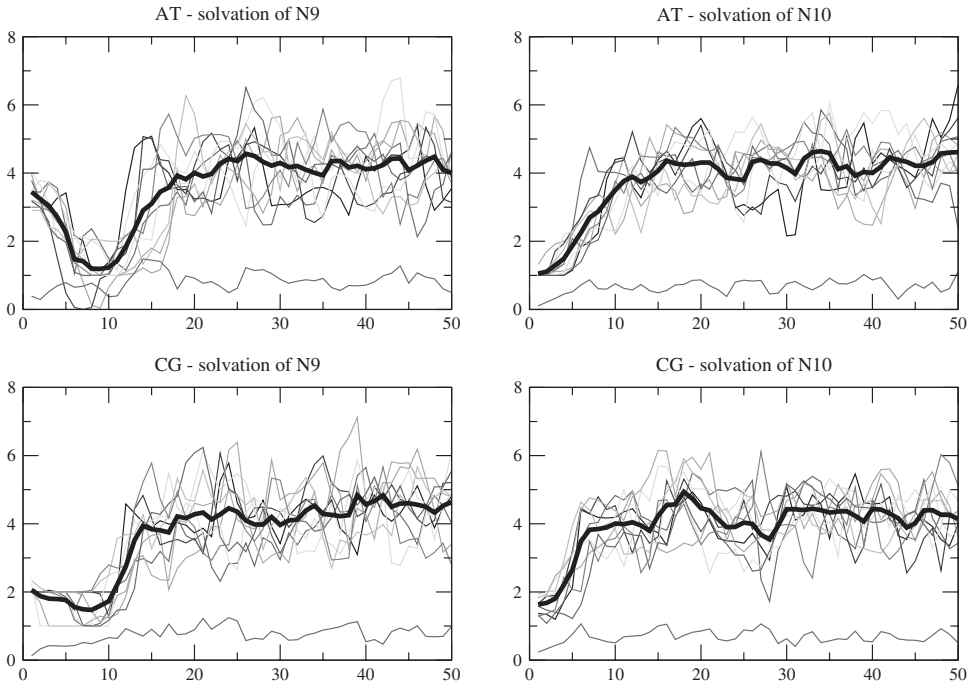

Figure 5. Dependence of the solvation coordination number on the pulling distance for N9 and N10 atoms in the 9-aminoacridine molecule. Pulling through the minor groove. The thick black curve in each plot is the average hydration coordination number. The thin curve at the bottom of each plot shows the standard deviation of the average. The *X* axis represents the distance of the BA atom from its initial position. The total displacement of BA during extraction of 9-AA was 50 Å.

Additionally, it can be seen that changes in the solvation pattern may be used as a criterion to determine the point at which the complex is disrupted. It can be noted that the plateau on the solvation profiles correspond well to the plateau on the force profiles. Attaining such a plateau means that the 9-aminoacridine molecule is totally pulled out from the DNA intercalation site and become fully solvated.

3. Stability of short α-helical polypeptides

3.1. Introduction

In another computer experiment we attempted to study the helical propensity of short polypeptides in aqueous solution using steered molecular dynamics simulations. Similarly to the procedure described above, used to study the intercalation process, we applied an external force to perform a stretching experiment for short polypeptides from their α-helical conformation to fully extended form in aqueous solution. We used NMe and Ace as blocking groups for the terminal residues and we chose 15 amino acids for the length of the simulated polypeptides.

The following sequences have been studied: polyalanine, polyglycine and polyvaline, as well as polyalanine with single amino acid in the middle of the chain substituted by glycine,

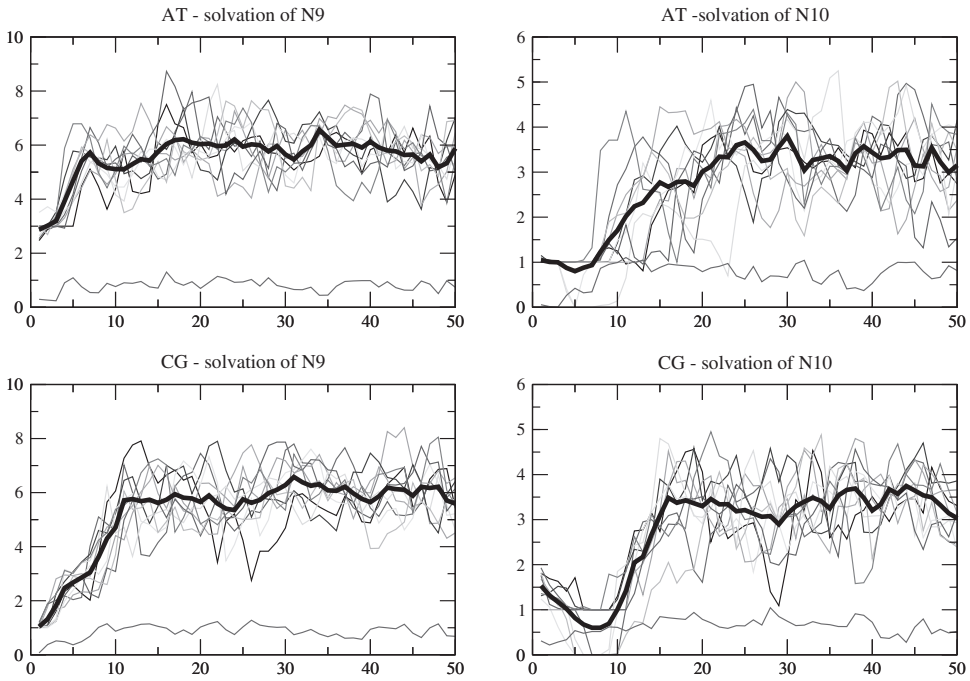

Figure 6. Dependence of the solvation coordination number on the pulling distance for N9 and N10 atoms in the 9-aminoacridine molecule. Pulling through the major groove. The thick black curve in each plot is the average hydration coordination number. The thin curve at the bottom of each plot shows the standard deviation of the average. The *X* axis represents the distance of the BA atom from its initial position. The total displacement of BA during extraction of 9-AA was 50 Å.

leucine or valine. According to various predictions [43] alanine has the largest value of helical propensity, while the helical propensity of valine is the lowest. Glycine is located somewhere in the middle on the helical propensity scales.

All simulations were performed in a periodic box of TIP3P [42] water molecules to solvate the whole system. The box was large enough to accommodate fully extended polypeptide. To perform the pulling experiment we attached an artificial BA atom to one end of the polypeptide in its α-helical conformation while keeping the last atom on the other end fixed. The stretching was performed by gradually moving the BA atom along the helical axis with the same velocity (50 m s^{-1}) as in the previous experiment, until the peptide affected its fully extended conformation (see figure 7). The total time of each simulation was 100 ps and the total size of the simulated system including water molecules was about 17 000 atoms in each case. We generated ten trajectories for each simulated system. The average force profiles for different sequences are presented in figure 8. All the polypeptide sequences studied here do not display any sequence specific behaviour. In contrast to what is well known experimentally, that the polyalanine short peptides have the highest helical propensity [43], the polyalanine studied here does not seem to be more or less stable than the other helices. Most probably the differences in the stabilities between various polypeptide sequences is masked by the fluctuations of the dominant solvent–solvent and solute–solvent forces, instead of intra-peptide interaction, which involves mainly hydrogen bonding and side chain interactions. The unnaturally large velocity

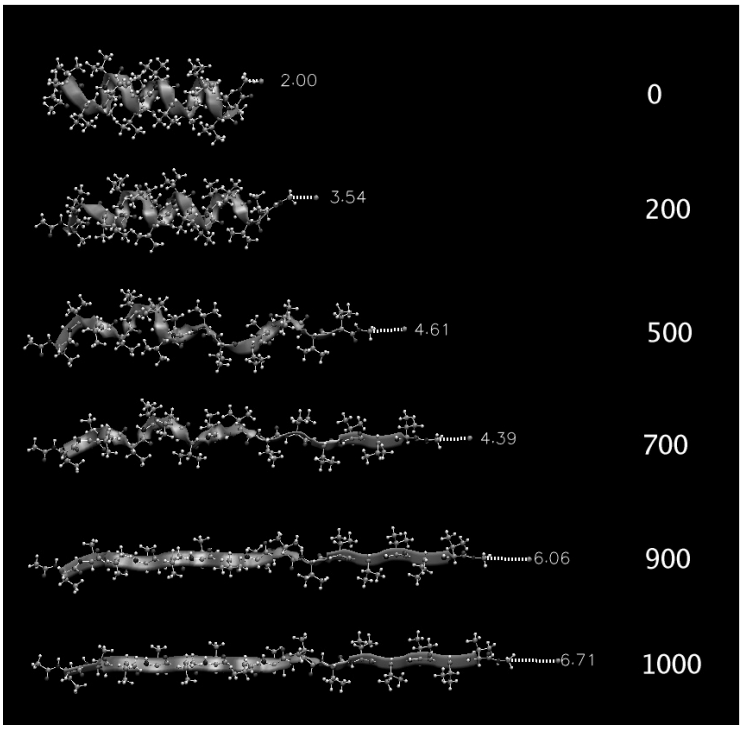

Figure 7. Image showing the transition from helix to coil. The bond between BA and an atom in polyalanine is drawn with a dotted line and the current length (in Å) is indicated. The elongation step is written next to each structure. In all simulations we performed 1000 steps of BA displacement.

of the artificial atom used to stretch the helices, which is several orders of magnitude larger than the one used under experimental conditions, causes dissipation of the energy, which is the other factor obscuring the minute differences in the energetics between the various amino-acid sequences. The trajectories generated in this study will be further analysed by implicit solvent approaches such as the MM/GBSA method [44], in order to better understand the role of various energy contributions during the stretching experiment.

4. Conclusions and perspectives

Our stretching experiments using a computational SMD method for the first time have provided a detailed microscopic description of the DNA intercalation process. The SMD technique provides qualitative results allowing the estimation of relative stabilities of the DNA–drug complexes. We think that the SMD technique together with other methods can be used to better understand the energetics of DNA–drug complex formation, and potentially can be used for designing pharmacologically active compounds. Our next goal is to perform a detailed energetic analysis using an MM/GBSA molecular dynamics trajectory post-processing technique [44] to decompose the total force and work into internal and solvent dependent components, as well as to determine the magnitude of entropy changes in SMD experiments.

In other computational experiments we attempted to measure the helical propensity of different amino acids. These demonstrated that it is difficult to handle explicit solvation effects in the SMD simulation, where forces between solute and solvent have a dominant contribution

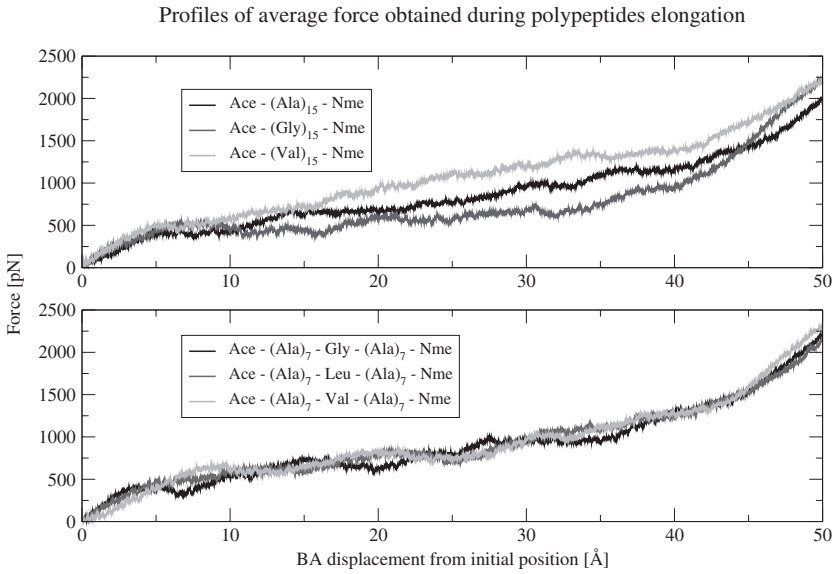

Figure 8. The force profiles obtained from pulling α-helices having different sequences of amino acids. The upper plot shows force profiles for helices consisting of the same amino acids. The lower plot shows profiles for helices built of alanine with middle residue replaced by glycine, leucine or valine. As can be seen, the profiles in the lower plot are almost indistinguishable, despite modifications in the amino acid sequences.

to the overall forces measured in the simulations. Work is underway to design a method to factor such an effect out from our results as well as to develop an approach that can be used to account for dissipative work in this type of computer experiments.

Acknowledgments

This research is supported by Polish State Committee for Scientific Research, grants 3 T09A 096 19 and 3 T09A 042 26. Plots in this article were created using Rasmol or VMD [45].

References

[1] Essevaz-Roulet B, Bockelmann U and Heslot F 1997 Mechanical separation of the complementary strands of DNA *Proc. Natl Acad. Sci. USA* **94** 11935–40

[2] Bockelmann U, Essevaz-Roulet B and Heslot F 1997 Molecular stick-slip revealed by opening DNA with piconewton force *Phys. Rev. Lett.* **79** 4489–92

[3] Strick T R, Allemand J-F, Bensimon D, Bensimon A and Croquette V 1996 The elasticity of a single supercoiled DNA molecule *Science* **271** 1835–7

[4] Allemand J-F, Bensimon D and Croquette V 2003 Stretching DNA and RNA to probe their interactions with proteins *Curr. Opin. Struct. Biol.* **13** 266–74

[5] Williams M C and Rouzina I 2002 Force spectroscopy of single DNA and RNA molecules *Curr. Opin. Struct. Biol.* **12** 330–6

[6] Florin E-L, Moy V T and Gaub H E 1994 Adhesion forces between individual ligand–receptor pairs *Science* **264** 415–7

[7] Moy V T, Florin E-L and Gaub H E 1994 Intermolecular forces and energies between ligands and receptors *Science* **266** 257–9

[8] Merkel R, Nassoy P, Leung A, Ritchie K and Evans E 1999 Energy landscapes of receptor–ligand bonds explored with dynamic force spectroscopy *Nature* **397** 50–3

[9] Kellermayer M, Smith S B, Granzier H L and Bustamante C 1997 Folding–unfolding transitions in single titin molecules characterized with laser tweezers *Science* **276** 1112–6
[10] Rief M, Gautel M, Oesterhelt F, Fernandez J M and Gaub H E 1997 Reversible unfolding of individual titin immunoglobulin domains by AFM *Science* **276** 1109–12
[11] Strick T R, Allemand J-F, Bensimon D and Croquette V 2000 Stress-induced structural transitions in DNA and RNA *Annu. Rev. Biophys. Biomol. Struct.* **29** 523–43
[12] Leckband D 2000 Measuring the forces that control protein interactions *Annu. Rev. Biophys. Biomol. Struct.* **29** 1–26
[13] Bustamante C, Bryant Z and Smith S B 2003 Ten years of tension: single-molecule DNA mechanics *Nature* **421** 423–7
[14] Izrailev S, Stepaniants S, Isralewitz B, Kosztin D, Lu H, Molnar F, Wriggers W and Schulten K 1998 Steered molecular dynamics *Computational Molecular Dynamics: Challenges, Methods, Ideas* (*Springer Lecture Notes in Computational Science and Engineering* vol 4) ed P Deuflhard, J Hermans, B Leimkuhler, A E Mark, S Reich and R D Skeel (Berlin: Springer) pp 39–65
[15] Izrailev S, Stepaniants S, Balsera M, Oono Y and Schulten K 1997 Molecular dynamics study of unbinding of the avidin biotin complex *Biophys. J.* **72** 1568–81
[16] Grubmüller H, Heymann B and Tavan P 1996 Ligand binding: molecular mechanics calculation of the streptavidin–biotin rupture force *Science* **271** 997–9
[17] Isralewitz B, Izrailev S and Schulten K 1997 Binding pathway of retinal to bacterio-opsin: a prediction by molecular dynamics simulations *Biophys. J.* **73** 2972–9
[18] Stepaniants S, Izrailev S and Schulten K 1997 Extraction of lipids from phospholipid membranes by steered molecular dynamics *J. Mol. Model.* **3** 473–5
[19] Jarzynski C 1997 Nonequilibrium equality for free energy differences *Phys. Rev. Lett.* **78** 2690–3
[20] Jarzynski C 1997 Equilibrium free-energy differences from nonequilibrium measurements: a master-equation approach *Phys. Rev.* E **56** 5018–35
[21] Fowler S B, Best R B, Herrera J L T, Rutherford T J, Steward A, Paci E, Karplus M and Clarke J 2002 Mechanical unfolding of a titin ig domain: structure of unfolding intermediate revealed by combining AFM, molecular dynamics simulations, NMR and protein engineering *J. Mol. Biol.* **322** 842–9
[22] Liphardt J, Dumont S, Smith S B, Tinoco I Jr and Bustamante C 2002 Equilibrium information from nonequilibrium measurements in an experimental test of Jarzynski's equality *Science* **296** 1832–5
[23] Park S and Schulten K 2004 Calculating potentials of mean force from steered molecular dynamics simulations *J. Chem. Phys.* **120** 5946–61
[24] Lantz M A, Jarvis S P, Tokumoto H, Martynski T, Kusumi T, Nakamura C and Miyake J 1999 Stretching the α-helix: a direct measure of the hydrogen-bond energy of a single-peptide molecule *Chem. Phys. Lett.* **315** 61–8
[25] Saenger W 1984 *Principles of Nucleic Acid Structure* (Berlin: Springer)
[26] Boye G L and Ampofo O 1983 Clinical uses of cryptolepis sanguinolenta *Proc. 1st Int. Seminar on Cryptolepine* ed K Boakye-Yiadom and S O A Bamgbose (Kumasi, Ghana: University of Kumasi) pp 37–40
[27] Lerman L S 1961 Structural considerations in the interaction of DNA and acridines *J. Mol. Biol.* **3** 18–30
[28] Nuss M E, Marsh F J and Kollman P A 1979 Theoretical studies of drug–dinucleotide interactions: empirical energy function calculations on the interaction of ethidium, 9-aminoacridine, and proflavin cations with base-paired dinucleotide gpc and cpg *J. Am. Chem. Soc.* **101** 825–33
[29] Cieplak P, Rao S N, Grootenhuis P D J and Kollman P A 1990 Free energy calculation on base specificity of drug–DNA interactions: application to daunomycin and acridine intercalation into DNA *Biopolymers* **29** 717–27
[30] Crenshaw J M, Graves D E and Denny W A 1995 Interactions of acridine antitumor agents with DNA: energies and groove preferences *Biochemistry* **34** 13682–7
[31] Berman H M, Olson W K, Beveridge D L, Westbrook J, Gelbin A, Demeny T, Hsieh S H, Srinivasan A R and Schneider B 1992 The nucleic acid database: a comprehensive relational database of three-dimensional structures of nucleic acids *Biophys. J.* **63** 751–9
[32] Berman H M, Westbrook J, Feng Z, Gilliland G, Bhat T N, Weissig H, Shindyalov I N and Bourne P E 2000 The protein data bank *Nucl. Acids Res.* **28** 235–42
[33] Maliniana L, Soler-Lopez M, Aymami J and Subirana J A 2002 Intercalation of an acridine-peptide drug in an AA/TT base step in the crystal structure of d(CGCGAATTCGCG)2 with six duplexes and seven Mg(2+) ions in the asymmetric unit *Biochemistry* **41** 9341–8
[34] Adams A, Guss J M, Collyer C A, Denny W A and Wakelin L P 1999 Crystal structure of the topoisomerase II poison 9-amino-[N-(2-dimethylamino)ethyl]acridine-4-carboxamide bound to the DNA hexanucleotide d(CGTACG)2 *Biochemistry* **38** 9221–33

[35] Zakrzewska K 2001 private communication, unpublished results
[36] Lu H and Schulten K 1999 Steered molecular dynamics simulations of force-induced protein domain unfolding *Proteins: Struct. Funct. Genet.* **35** 453–63
[37] Pearlman D A, Case D A, Caldwell J W, Ross W R, Cheatham T E III, DeBolt S, Ferguson D, Seibel G and Kollman P 1995 AMBER, a computer program for applying molecular mechanics, normal mode analysis, molecular dynamics and free energy calculations to elucidate the structures and energies of molecules *Comput. Phys. Commun.* **91**
[38] Kamitori S and Takusagawa F 1992 Crystal structure of the 2:1 complex between d(GAAGCTTC) and the anticancer drug actinomycin D *J. Mol. Biol.* **225** 445–56
[39] Wang J, Cieplak P and Kollman P A 2000 How well does a restrained electrostatic potential (RESP) model perform in calculating conformational energies of organic and biological molecules? *J. Comput. Chem.* **21** 1049–74
[40] Bayly C I, Cieplak P, Cornell W D and Kollman P A 1993 A well-behaved electrostatic potential based method using charge restraints for determining atom-centered charges: the RESP model *J. Phys. Chem.* **97** 10269–80
[41] Frisch M J, Trucks G W, Schlegel H B, Scuseria G E, Robb M A, Cheeseman J R, Zakrzewski V G, Montgomery J A Jr, Stratmann R E, Burant J C, Dapprich S, Millam J M, Daniels A D, Kudin K N, Strain M C, Farkas O, Tomasi J, Barone V, Cossi M, Cammi R, Mennucci B, Pomelli C, Adamo C, Clifford S, Ochterski J, Petersson G A, Ayala P Y, Cui Q, Morokuma K, Malick D K, Rabuck A D, Raghavachari K, Foresman J B, Cioslowski J, Ortiz J V, Baboul A G, Stefanov B B, Liu G, Liashenko A, Piskorz P, Komaromi I, Gomperts R, Martin R L, Fox D J, Keith T, Al-Laham M A, Peng C Y, Nanayakkara A, Challacombe M, Gill P M W, Johnson B, Chen W, Wong M W, Andres J L, Gonzalez C, Head-Gordon M, Replogle E S and Pople J A 1998 *Gaussian 98* Revision A.9 (Pittsburgh, PA: Gaussian Inc.)
[42] Jorgensen W L, Chandrasekhar J, Madura J D, Impey R W and Klein M L 1983 Comparison of simple potential functions for simulating liquid water *J. Chem. Phys.* **79** 926–36
[43] Pace C N and Scholtz J M 1998 A helix propensity scale based on experimental studies of peptides and proteins *Biophys. J.* **75** 422–7
[44] Kollman P A, Massova I, Reyes B, Kuhn C, Huo S, Chong L, Lee M, Lee T, Duan Y, Wang W, Donini O, Cieplak P, Srinivasan J, Case D A and Cheatham T E III 2000 Calculating structures and free energies of complex molecules: combining molecular mechanics and continuum models *Acc. Chem. Res.* **33** 889–97
[45] Humphrey W, Dalke A and Schulten K 1996 VMD—Visual Molecular Dynamics *J. Mol. Graph.* **14** 33–8